16th Australasian Fluid Mechanics Conference
Crown Plaza, Gold Coast, Australia
2-7 December 2007

Numerical Investigation of a Small Gas Turbine Compressor

J. Ling, K.C. Wong & S. Armfield

School of Aerospace, Mechanical & Mechatronic Engineering
University of Sydney, NSW, 2006 AUSTRALIA

Abstract

This paper presents the initial development and study of a centrifugal compressor undertaken at the Micro Propulsion Group (MPG), University of Sydney. The compressor is used in a small gas turbine engine (108mm diameter). Gerendás et al [1] refer to gas turbines of this size as small aero-engines. The gas turbine chosen for the initial study is the KJ66, which is one of the most robust and primitive small gas turbine designs available.

This project is aimed at improving the performance and efficiency of a KJ66 small gas turbine, which currently utilises a 66mm diameter centrifugal impeller and radial wedge type diffuser. The proposed replacement impeller is 71mm diameter, coupled to a mixed flow vaned diffuser to produce a higher pressure ratio at design conditions. The changes were made in such a way that the original engine's diameter of 108mm was maintained. The geometry of the diffuser vanes was redesigned to ensure effective diffusion, while directing the flow from the radial to axial direction in a smooth turn. In addition to increasing the impeller diameter, having smooth turns in the stage components is expected to increase compression efficiency, at least in a certain operational range.

The work presented here uses Computational Fluid Dynamics (CFD) simulations. The performance and efficiency charts of the original compressor stage, with a KKK2038 compressor wheel coupled to a wedge-type diffuser, were mapped. The performance chart of the new design was also mapped and comparisons are made. The performance of the new stage design is notably better than the original design, within a certain operational range. The power requirement to drive the compressor was also checked to ensure its compatibility with the turbine drive.

Nomenclature

η	Efficiency
P	Pressure
k	Specific air ratio
Pr	Pressure ratio
μ	Work Coefficient
W	Work
h	Enthalpy
M	Mach Number
C	Absolute flow velocity
U	Impeller local tangential speed
C_p	Constant pressure specific heat

Subscripts

t	Total condition
th	Thermal properties
tt	Total to total conditions
00	Stagnation to stagnation conditions
1	Impeller inlet conditions
2	Impeller tip conditions
θ	Tangential component

Introduction

The application of small gas turbine engines ranges from hobbyist model jet aircrafts to target drones, and Unmanned Aerial Vehicles (UAV). Due to the low efficiency and thrust-to-weight ratio, they are limited to short range applications. However, the inability for spark ignition engines to work at high altitude warrants further development to improve the efficiency of these miniature gas turbines. Furthermore, gas turbines in the form of turbojet or turbofan are capable of providing propulsion at higher speed, where spark ignition engines are not applicable with air screws.

Most small gas turbines for aero-propulsion use centrifugal compressors similar to those from automotive turbochargers. The dissimilarity is that turbochargers usually have their radial diffuser coupled to a volute with delivery outlet tangential to the rotor, while aero engines do not benefit from this design due to space and design restrictions. The inlet and outlet of small aero engines such as the KJ66 are both axial even though the compressor wheel is of a centrifugal type. The passage turns immediately after the diffuser into the axial direction, to feed pressurised air into the combustion chamber right behind the compressor (Figure 1).

The ideal thermal efficiency of a gas turbine is related to the pressure ratio and can simply be estimated by a well-known equation [2]:

$$\eta_{th} = 1 - \frac{1}{\left(P_2/P_1\right)^{k-1/k}} \tag{1}$$

In such small engines the ideal thermal efficiency ranges between 10 and 20%. However, losses due to the nature of these engines running at high rotational speed and high flow velocity relative to the size of air passages plague these engines, further lowering the efficiency. Due to the small diameter, the compressor rotors have to run at nominal speeds of around 100,000 rpm. At this speed, a 10cm diameter engine (with 62~68mm impeller wheel and a diffuser section which makes up the rest of the diameter) can only produce a pressure ratio of around 1.8 ~ 2. This is normally achieved by incorporating a centrifugal compressor due to the fact that they are more compact compared to axial machines and capable of achieving a higher pressure ratio per stage. The high rotational speed also gives high frictional losses in mechanical parts.

It is therefore proposed to improve the engine by redesigning the compressor so that it will produce a higher pressure ratio and run at lower speeds, if possible. However, the pressure rise is proportional to the square of impeller tip Mach number [3]

$$\mathrm{Pr}_{tt} = \left(1 + (k-1)\eta\mu M_{U2}^2\right)^{k/(k-1)} \tag{2}$$

In other words, to maximise performance-to-rotational speed ratio, the diameter of the compressor wheel must be increased to maintain the tip speed, while the rotational speed reduced.

However, within the space constraints of the small engine, this can only be achieved by compromising the diffuser section design.

The diffuser is necessary to recover the kinetic energy of the flow and transform it into pressure. The diverging rate must be correctly designed within the working range to ensure high efficiency conversion of kinetic energy. If a larger compressor wheel is employed, there is not much space left for the diffuser section.

Fortunately, compressors in aero-engines do not need wide mass flow range at a specific rpm when compared to industrial compressor systems or automotive turbochargers. Therefore only the performance in a certain range is necessary to be improved. It should be noted that this compressor is driven by an axial turbine through a direct shaft. This enables control of the flow by selection of an appropriately sized turbine, so that the compressor will only work within the matched range. This allows us to have a diffuser section designed in such a way that the performance is altered to give a head-to-flow curve more similar to an axial stage.

Centrifugal stages have flat head-to-flow curve, while axial stages have a steep curve. Axial stages usually have much higher flow rates compared to a centrifugal stage of similar diameter [5]. In a compact engine such as the KJ66, a centrifugal stage is chosen due to the compactness and higher stage pressure ratio. The proposed centrifugal stage design achieves a higher pressure ratio at lower flow rate, but with a rapidly reduced pressure ratio with higher flow rates. Under such circumstances it may likely necessary to redesign the turbine stage (which is not a subject of discussion in this publication) to ensure the mass flow rate always falling within the optimised range.

To accommodate a larger compressor wheel, the original radial wedge type diffuser no longer performs well; there is no longer enough radial distance to form diffuser passages with the required divergence rate. Therefore a vaned diffuser section which gradually guides the air into the axial direction while the passage expands was designed, requiring a careful selection of the radial-to-axial curvature to minimise separation and recirculation. After several attempts, a decision was made to increase the size of the impeller wheel to 71mm so that a diffuser of correct turning rate could be accommodated.

Original Compressor Stage

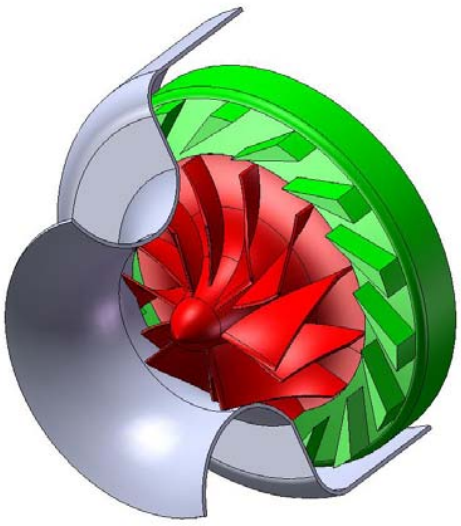

Figure 1: 3D model of original stage design of KJ66.

The original design of the compressor stage in the KJ66 has a 66mm compressor wheel coupled to a radial wedged diffuser section (Figure 1). The flow is turned from radial to axial immediately after the diffuser passages. The wedge section is positioned at an angle of 3° to the radial. The inner diameter of the casing is 107.4mm.

The aerodynamic design of the compressor wheel normally starts with 1D equations and is correlated with empirical data [4]. The geometry data from initial 1D analysis is then used to produce a physical geometry for the wheel, defined by a series of curves. With the help of some simple measuring devices and the compressor design software ANSYS BladeModeller, the geometry of the KKK2038 compressor wheel was digitally reproduced. The performance of the compressor stage from 1D analysis agrees well with the manufacture's specification for maximum rpm. The impeller tip diameter is 66mm, with inlet hub and inlet shroud diameters 12.5mm and 45mm respectively. The blade geometry definition is shown in Figure 2. A clearance of 0.3mm between the shroud tip and the casing was modelled.

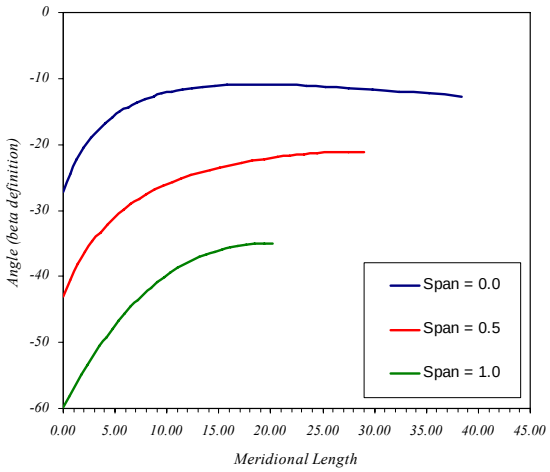

Figure 2: Impeller blade angle definition

CFD Model of Original Stage

The CFD results were obtained using CFX commercial CFD package. Only one passage of each of the impeller and diffuser sections was meshed for the simulations. A rotational periodic boundary condition was applied.

Meshes for the impeller domain and the diffuser domain were generated independently. The mesh of the impeller domain was generated using ANSYS Turbogrid and contained only hexahedra elements; while the diffuser section was meshed using CFX-mesh with tetrahedral/prism elements.

Table 1: Mesh information

Domain	Nodes	Elements
Impeller	110170	99705
Diffuser	18292	46071
All Domains	128462	145776

The two domains were connected by a General Grid Interface (GGI) with non matching grid, which iterates and checks balances in fluxes. Steady state solutions were obtained using the k-ε model. Although it does not show the flow details such as flow separations, grid independence studies showed this would be sufficient to obtain accurate performance curves.

Total pressure inlet and mass flow outlet boundary conditions were chosen so that the solutions for a range of mass flows could be obtained. The inlet turbulence intensity was set to be 3% with the length scale auto-computed by CFX. The inflow vector was set to be axial to the rotational axis with a stationary frame total temperature of 300K. The entire computational volume of the impeller passage was placed in a rotational frame except the inlet face and the shroud surface.

Both stationary and moving walls were modelled as smooth non-slip walls. The mesh generation method was based on a boundary layer with 0.1mm layer thickness, expansion rate of 1.33 and a 0.002mm wall offset. Mesh details are given in Table 1. All residuals were required to be converged to at least 1.0e-4, with high efficiency points converged to 1.0e-6.

Results of Original Stage

Pressure ratio and efficiency curves for the original stage running at 80,000, 100,000, 117,000 and 120,000 rpm are shown in Figure 3. The specification of the KJ66 engine states the maximum speed of the engine is 117,000rpm, at which the compressor produces a pressure ratio of 2.2 at a flow rate of 0.22kg/s. This is well matched by the results from CFD simulations as shown.

Both Figure 3 and Figure 4 show the pressure and efficiency curve features of typical centrifugal compressors, where pressure and efficiency peak at a certain flow rate. Increasing or decreasing the flow rate from this optimum point results in a reduction in both pressure and efficiency. Pressure drops rapidly with the increase in mass flow rate and this will lead to chocking at a certain point. On the other hand, pressure also drops accordingly as the mass flow rate is reduced from that optimum point and the stage will quickly start to surge. The exact points for surging and choking would not be predicted.

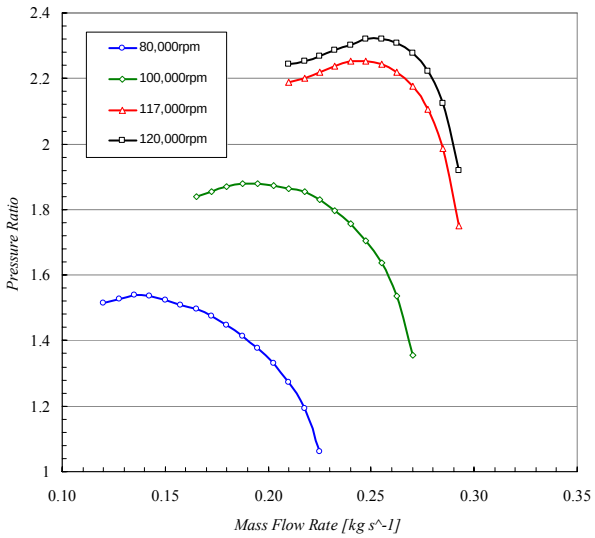

Figure 3: Pressure ratio – mass flow curve of the compressor stage.

Total isentropic properties are used for the efficiency definition in this case, as both pressure and velocity at the stage outlet are a useful form of energy in a gas turbine. Kinetic energy in the flow which is not yet transformed into pressure, can be used to enhance mixing in the combustion process or used to build up more pressure later by further diffusion. Total isentropic efficiency is then defined by

$$\eta_{isen} = \frac{\Delta h_t}{W_{input}} \qquad (3)$$

It is expected the actual efficiency will be lower than the simulation results shown in Figure 4 due to minor losses, such as heat loss through the casing and mechanical friction, (which were not taken into account in the modelling). But the efficiency curves still show the correct trend, which is sufficient for comparative studies.

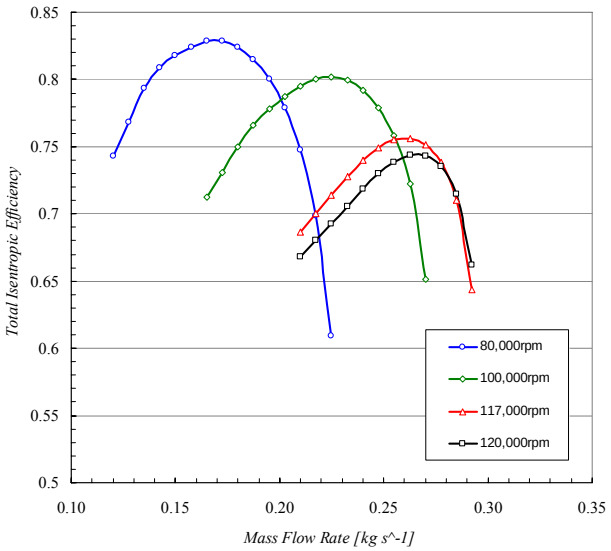

Figure 4: Stage efficiency curves.

Figure 4 shows the efficiency of the stage drops as the speed increases from 80,000rpm to 120,000rpm. Even though the stage is capable of producing a higher pressure ratio, it has limitations in flow rate and the efficiency will drop accordingly.

New Compressor Design

The improved design of the compressor stage incorporates a 71mm impeller wheel with a larger inlet flow area and a mixed flow diffuser section with rounded turn. The 71mm impeller wheel alone was designed to give higher mass flow. However, this diffuser section which turns the air 90° does not work very well with higher flow velocity. Earlier trial and error investigations showed that if the flow velocity is too high, which is often the case for flow leaving the impeller outlet at a high flow rate; the flow in the diffuser section separated quickly and formed an aerodynamic blockage.

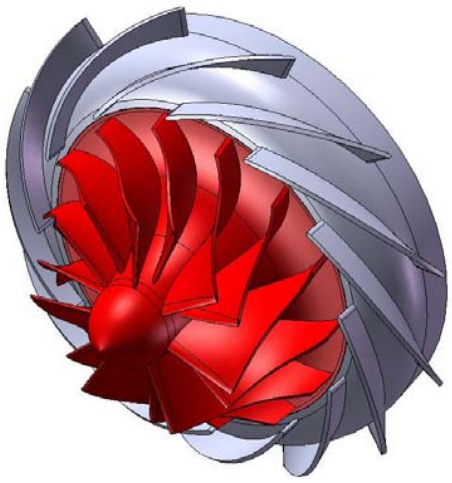

Figure 5: 3D model of the new compressor stage incorporate 71mm impeller wheel

Unlike the radial wedge diffuser, where the flow velocity was already slowed down before it entered the turn, the mixed flow diffuser slows the flow while making the turn simultaneously. Therefore either the volumetric flow rate or the impeller tip velocity needed to be reduced before the flow turns into the axial direction. The higher tip backswept angle on the 71mm impeller blade is designed to lower the absolute flow velocity leaving the impeller outlet.

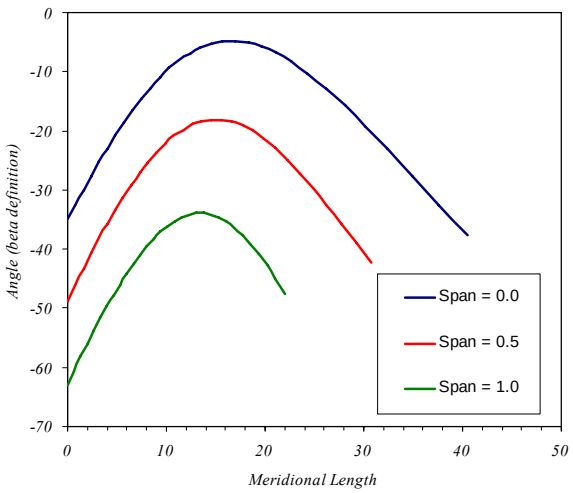

Figure 6: Impeller blade angle definition (71mm wheel)

Figure 6 shows the new compressor has blades with a higher backswept angle. The inlet hub and shroud diameters are increased to 18mm and 56mm respectively. The impeller blade tip height in this case was increased from 6mm in the original impeller to 6.2mm.

In the diffuser section, the passages are separated by vanes instead of wedges, to control the rate of diffusion while making the turn into axial direction. Without increasing the overall engine diameter, the diffuser makes a smooth turn within a shorter distance while maintaining the engine's 107.4mm inner diameter. The angle of the diffuser vanes is approximately linear (Figure 7), with an inlet angle of 70°, which was determined by earlier CFD simulations for flows in the impeller passages alone.

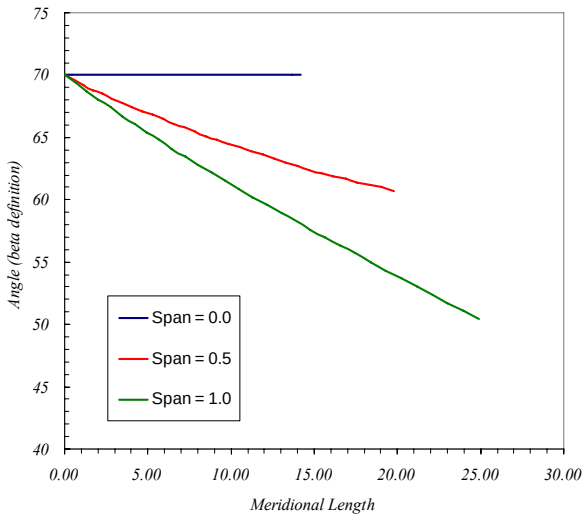

Figure 7: Diffuser blade angle definition.

CFD Model of New Design

The CFD model of the stage with a 71mm impeller wheel was meshed similarly to that of original design, as discussed earlier. The only difference was that the geometrical nature of the vaned diffuser enabled the section to be meshed with hexahedra elements providing greater computational efficiency. Mesh details are given in Table 2. Simulations were made with the stage running at 100,000rpm and 120,000rpm.

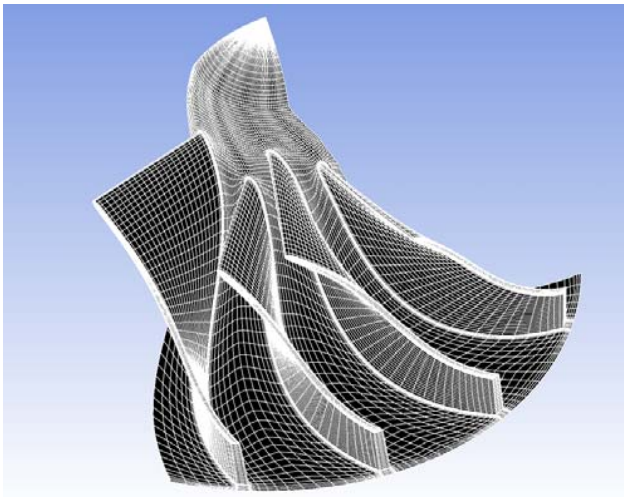

Figure 8: Hexahedra mesh on the 71mm impeller wheel (showing two passages).

Table 2: Mesh information of new compressor stage.

Domain	Nodes	Elements
Impeller	141156	128926
Diffuser	59997	63760
All Domains	201153	182686

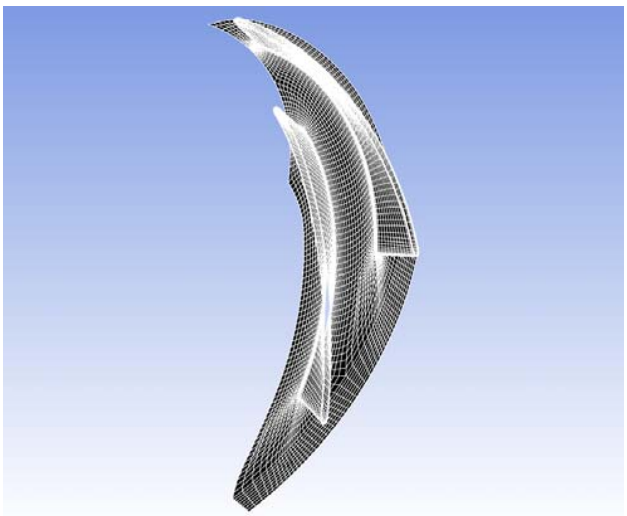

Figure 9: Hexahedra mesh on the diffuser passage (showing two passages).

Results of New Design

Simulation results showed the new design did not produce higher flow rates when coupled to the vaned diffuser, despite the increased inlet eye diameter. At 100,000rpm, the pressure ratio drops rapidly as the flow rate is increased and the new design gives a lower pressure ratio than the original compressor when the flow rate exceeds 0.228kg/s (Figure 10). Even with the

impeller operating at 120,000rpm it is not expected to give higher mass flow rate compared to the original stage.

A similar trend is observed in the efficiency plot (Figure 12). At 100,000rpm, efficiency drops below the efficiency of the old stage at 0.225kg/s flow rate.

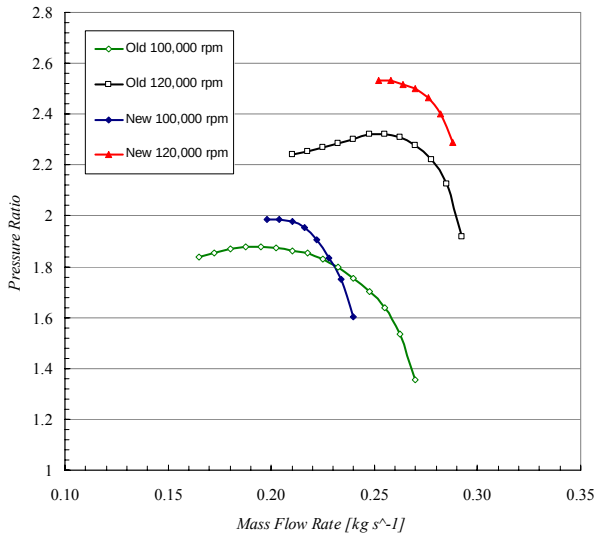

Figure 10: Pressure ratio curves for new design compared to the old design.

The rapid performance degradation at higher flow rates may be related to the increase in recirculation in the turning section of the diffuser. Figure 11 shows the velocity distribution is more even at the outlet with the lower mass flow rate (b), compared to the velocity contour for higher mass flow rate (a).

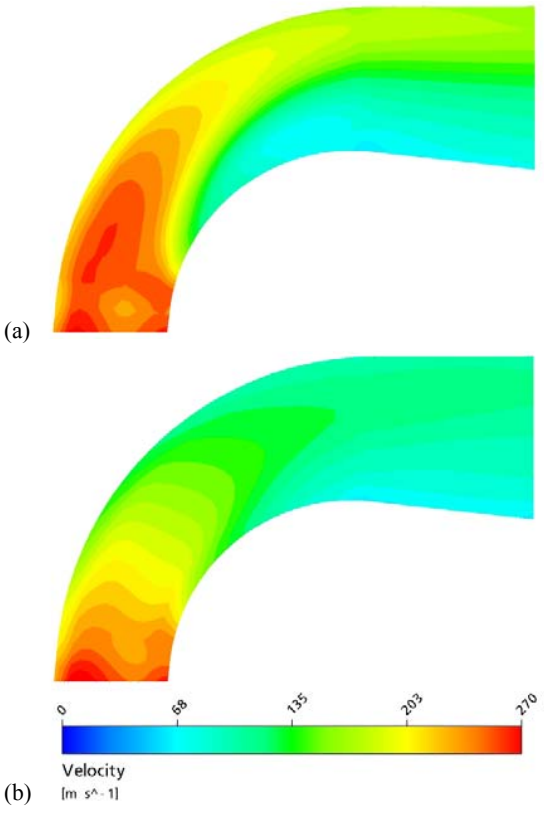

Figure 11: Meridional velocity contours in the diffuser with flow rate (a) 0.228kg/s, and (b) 0.186kg/s, with the impeller operating at 100,000rpm.

The main improvement over the old design is the pressure ratio at a lower mass flow rate. At this lower end, both pressure and efficiency are significantly higher than those of the original stage. Unlike compressors in industrial applications, where the flow rate of a stage is controlled by a separate system such as an electric motor, the mass flow rate in a gas turbine depends on a well-matched turbine, connected by a common shaft, with the mass flow increasing proportionally with the rpm. Therefore, with a correctly matched turbine, the flow rate could be controlled within the optimised range.

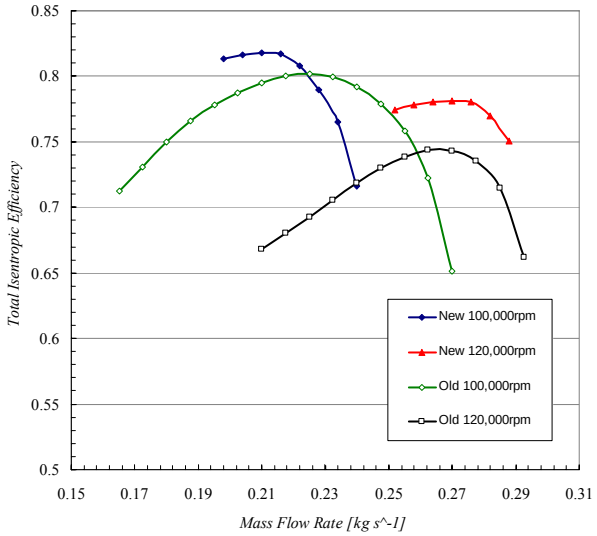

Figure 12: Efficiency curves of new design compared to ole ones

Discussion and Conclusion

CFD simulations show the pressure ratio and efficiency of the compressor stage were significantly enhanced at the operational flow rate of the engine at corresponding rpm, by utilising a larger impeller wheel and a rounded turn in the diffuser section.

With larger inlet flow area on the 71mm impeller wheel, the impeller allows more mass flow. This will allow flat pressure ratio curves to extend further into higher mass flow regime with a radial diffuser configuration. However, the larger inlet mean radius does not help give a higher pressure ratio. Equation (2) can also be written as

$$\mathrm{Pr}_{tt} = \left(1 + \frac{\eta}{C_p T_{00}}\left(U_2 C_{\theta 2} - U_1 C_{\theta 1}\right)\right)^{k/(k-1)} \qquad (4)$$

With a larger inlet mean radius, the velocity term $U_1 C_{\theta 1}$ is relatively large and therefore reduces the pressure ratio according to Equation (4). However, as the engine does not require higher flow rate, as well as the fact the new vane diffuser was not designed to do so, the inlet hub and shroud diameters can be reduced. This will allow a higher pressure build up at the impeller exit.

Figure 13 shows the power requirement of the new stage compared to the original one running at 100,000rpm and 120,000rpm. At lower flow rates there is no significant increase in power requirement. Therefore, it is likely the original turbine of the KJ66 (maximum flow rate of 0.22kg/s at 117,000rpm) will match acceptably well with this new compressor stage.

Proposed future work includes detailed CFD analysis using k-ω turbulence model with SST wall model. This will enable studies of flow separation and recirculation in the diffuser section and their correlation to the overall performance. Also, studies of the effect of having diffuser sections of different turning radii will be

undertaken to determine whether it is possible to utilise an even larger impeller wheel or reduce the engine's diameter. A compressor wheel of 71mm diameter but with lower flow coefficient will also be tested with the rounded diffuser section.

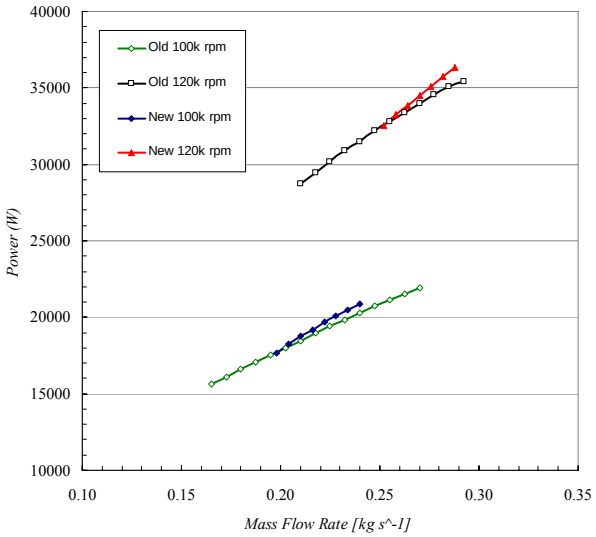

Figure 13: Power requirement of the compressor.

References

[1] M. Gerendás & R. Pfister, Development of a very small aero-engine. *45th ASME International Gas Turbine and Aeroengine Technical Congress and Exposition. Procedings of the ASME Turbo Expo 2000.*

[2] R. Sonntag, C. Borgnakke & G. Van Wylen, *Fundamentals of Thermodynamics, 5th Ed John Wiley & Sons 1998*

[3] D. Japikse, *Centrifugal Compressor Design and Performance, Concepts ETI Inc 1996*

[4] D. Japikse & N. Baines, *Introduction to Turbomachinery, Concept ETI 1994*

[5] R. Aungier, *Centrifugal Compressors: A Strategy for Aerodynamic Design and Analysis*, *ASME 2000*

[6] D. Flaxington & E. Swain. *Turbocharger Aerodynamic Design. Proc Instn Mech Engrs 1999 Vol 213 Part C. pp.43-57*

[7] P. Dalbert, B. Ribi, T. Kmeci & M.V. Casey. *Radial Compressor Design for Industrial Compressor. Proc Instn Mech Engrs 1999 Vol 213 Part C. pp.71-83*

[8] P.M. Came & C.J. Robinson. *Centrifugal Compressor Design. Proc Instn Mech Engrs 1999 Vol 213 Part C. pp.139-155*

[9] A. Lohmberg, M. Casey & S. Ammann. Transonic Radial Compressor Inlet Design. *Proc Instn Mech Engrs 2003 Vol 217 Part A. pp.367-374*

[10] J.D Denton & W.N. Dawes. Computational Fluid Dynamics for Turbomachinery Design. *Proc Instn Mech Engrs 1999 Vol 213 Part C. pp.107-124*

[11] R. Aghaei Tog, A. Mesgharpoor Tousi & M. Soltani. *Design and CFD Analysis of Centrifugal Compressor for a Microgasturbine. Aircraft Engineering & Aerospace Technology: An International Journal 79/2 (2007) 137-143*

[12] S. Ibaraki, T. Matsuo, H. Kuma, K. Sumida & T. Suita. *Aerodynamics of a Transonic Centrifugal Compressor Impeller. Transactions of the ASME J. Turbomachinery 2003 Vol 125 pp. 346-351*

[13] ANSYS CFX, Release 11.0, ANSYS Inc. Southpointe December 2006.